Buckling analysis of SMA bonded sandwich structure – using FEM

Pankaj V Katariya*, Arijit Das, Subrata K Panda

Department of Mechanical Engineering, NIT Rourkela, Rourkela-769008, Odisha, India.

E-mail: pk.pankajkatariya@gmail.com

Abstract. Thermal buckling strength of smart sandwich composite structure (bonded with shape memory alloy; SMA) examined numerically via a higher-order finite element model in association with marching technique. The excess geometrical distortion of the structure under the elevated environment modeled through Green's strain function whereas the material nonlinearity counted with the help of marching method. The system responses are computed numerically by solving the generalized eigenvalue equations via a customized MATLAB code. The comprehensive behaviour of the current finite element solutions (minimum buckling load parameter) is established by solving the adequate number of numerical examples including the given input parameter. The current numerical model is extended further to check the influence of various structural parameter of the sandwich panel on the buckling temperature including the SMA effect and reported in details.

1. Introduction

The demand for the lighter and stronger materials has been increasing day by day in many aerospace and automotive industries. The structure as well as structural components of such industries experience the combined types of loadings (aerostatic, dynamic and aerodynamic heating) during their life cycle and are prone to buckle and can lose their stability because of the large geometrical distortion. Hence, the structural instability becomes a foremost concern in safe and reliable designs. The sandwich material strengthens via incorporating the Shape Memory Alloy (SMA) fibre, is one of the potential materials (ability to recover extremely large strains) which can handle such difficulties and perform the necessary function satisfactorily.

The buckling behaviour of the laminated as well as sandwich layered structures are studied by various researchers using different theories and few essential contributions in this field are presented here to establish the necessity of the current analysis. The finite element (FE) technique is adopted in the past [1-3] to investigate the structural responses (bending, vibration, buckling, post-buckling and acoustic) of SMA embedded composite structure of various geometries under the elevated thermal environment with the help of von-Karman strain-kinematics. Similarly, the static and the dynamic responses of SMA bonded structure are computed numerically as well as the experimental techniques [4] and compared with previously available 1-D models (Tanaka, Rogers, Liang and Brinson). The bifurcation type of buckling responses of the sandwich structure evaluated by Shiau and Kuo [5] using the higher-order triangular element for the sake of high-accuracy. Subsequently, the FE solutions of the nonlinear frequency values of SMA bonded layer composite structure obtained [6] via the first-order shear deformation theory (FSDT) and von-Karman nonlinear strain. In the recent past, the finite element method (FEM) is adopted to explore the buckling behaviour of the SMA fibre embedded composite structure [7-8] using the polynomial based mid-plane theories (FSDT and 3-D layer-wise theory; LWT). The first time, the higher-order shear deformation theory (HSDT) and Green-Lagrange strain-displacement relations are adopted by Panda and Singh [9] to compute the nonlinear fundamental frequencies of the SMA embedded layer composite spherical panel numerically

using the FEM in association with the direct iterative method. Further, the sandwich plate structure bonded with SMA fibre modeled via Carrera's Unified Formulation (CUF) by Dehkordia and Khalili [10] for the frequency analysis using FEM technique and Kirchhoff's plate theory. Recently, the FEM technique in conjunction with the HSDT is adopted by Katariya *et al*. [11] to examine the buckling responses of SMA embedded sandwich shell panel structures including the geometrical nonlinearity via Green-Lagrange strain kinematics.

The review indicates that an extensive amount of study has already been reported on the buckling strength of the layered composite structure bonded with or without SMA fibres. Moreover, the reported studies are mainly utilized the FSDT kinematic model and von-Karman strain. Based on the authors' knowledge no study reported yet on the thermal buckling responses of SMA embedded sandwich structure via HSDT kinematics and Green's nonlinear strain-displacement relations. Hence, the current research aims to compute thermal buckling load parameter of SMA embedded sandwich flat panel structure numerically via the HSDT kinematics including the Green-Lagrange nonlinear strain and through thickness stretching effect. In order to compute the responses, a customized computer code (MATLAB environment) derived using the presently developed higher-order nonlinear FE model. The corresponding eigenvalue equation is derived by minimizing the total potential energy functional. After the necessary checking of the current numerical solution, it is engaged to compute the thermal load parameter of the layered sandwich structure bonded with and without SMA fibre and the final parametric (length-to-thickness ratio, aspect ratio and core-to-face thickness ratio) inferences discussed in details.

2. Mathematical modelling

The sandwich composite plate embedded with SMA fibre is considered here for the analysis purpose and Figure 1 represents the structural geometry. The geometrical dimension of the sandwich plate length, width and total thickness are represented as '*a*', '*b*' and '*h*', respectively. In addition, the total thickness is the sum of two components i.e., core thickness 'h_c' and face sheet thickness 'h_f'.

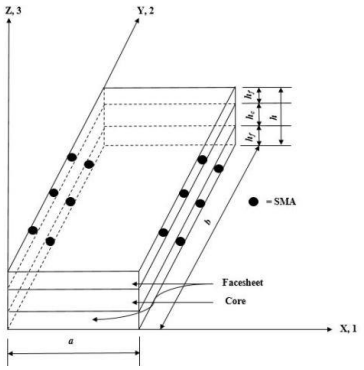

Figure 1. Configuration of the SMA embedded sandwich laminated composite plate

The higher-order displacement field kinematics [11] is adopted for the current modeling of layered sandwich panel embedded with SMA fibre and each node has ten degrees-of-freedoms (DOFs) per node. The panel model expressed mathematically in the following form as in Katariya *et al.* [11]:

$$\left.\begin{aligned}\bar{u} &= u_0 + z\theta_1 + z^2\phi_1 + z^3\zeta_1\\ \bar{v} &= v_0 + z\theta_2 + z^2\phi_2 + z^3\zeta_2\\ \bar{w} &= w_0 + z\theta_3\end{aligned}\right\} \tag{1}$$

where, $(\bar{u},\bar{v},\bar{w})$ represents the displacement and (u_0,v_0,w_0) represents the mid-plane displacement of any point within the plate component along the principal material direction i.e. 1, 2 and 3, respectively. The rotation of normal to the mid-plane to the alternate axes represented as θ_1 and θ_2, respectively whereas θ_3 is the stretching through the thickness. Similarly, a few extra mathematical functions (Taylor's series expansion) i.e. $\phi_1,\phi_2,\zeta_1,$ and ζ_2 required to maintain the necessary stress profile for the sandwich panel.

The generalised strain-displacement relations utilised for the present SMA embedded layered sandwich plate structure as in Katariya *et al*. [11]:

$$\left.\begin{aligned}\left\{\varepsilon_{Total}\right\} &= \left\{\varepsilon_{11} \quad \varepsilon_{22} \quad \varepsilon_{33} \quad \gamma_{23} \quad \gamma_{13} \quad \gamma_{12}\right\} \\ &= \left\{\frac{\partial u}{\partial x}+\frac{w}{R_1} \quad \frac{\partial v}{\partial y}+\frac{w}{R_2} \quad \frac{\partial w}{\partial z} \quad \frac{\partial v}{\partial z}+\frac{\partial w}{\partial y}+2\frac{w}{R_{12}} \quad \frac{\partial u}{\partial z}+\frac{\partial w}{\partial x}-\frac{u}{R_1} \quad \frac{\partial u}{\partial y}+\frac{\partial v}{\partial x}-\frac{v}{R_2}\right\}\end{aligned}\right\} \tag{2}$$

The required elastic constants associated with the SMA fibre and the composite are defined in Figure 1, along with the corresponding directions of the plate structure. Additionally, a uniform distribution of SMA including the close bonding with composite lamina is assumed throughout the analysis. The necessary elastic constants of SMA fibre within the plate structure are defined as same as in Panda and Singh [9]:

$$\left.\begin{aligned}&E_1 = E_{1m}V_m + E_sV_s, E_2 = \left(1\Big/\frac{V_s}{E_s}+\frac{V_m}{E_{2m}}\right) \\ &G_{12} = \left(1\Big/\frac{V_s}{G_s}+\frac{V_m}{G_{12m}}\right), G_{23} = G_{23m}V_m + G_sV_s \\ &\upsilon_{12} = \upsilon_{12m}V_m + \upsilon_sV_s, \alpha_2 = \alpha_{2m}V_m + \alpha_sV_s \\ &\alpha_1 = \left(\left(1\Big/\left(\frac{1}{\alpha_{1m}}+\frac{E_sV_s}{E_{1m}\alpha_{1m}V_m}\right)\right)+\left(1\Big/\left(\frac{E_{1m}V_m}{E_s\alpha_sV_s}+\frac{1}{\alpha_s}\right)\right)\right)\end{aligned}\right\} \tag{3}$$

Here, the subscripts '*s*' and '*m*' indicate the SMA fibre and the composite matrix, respectively. Similarly, '*E*' (elastic constant), '*G*' (rigidity modulus), 'υ' (Poisson's ratio) and 'α' (linear thermal expansion co-efficient) are the necessary input material parameter assumed according to the analysis. Additionally, the corresponding volume fractions of the matrix material and the SMA fibre shown in Eq. (3) defined as 'V_m' and 'V_s', respectively.

Further, the thermoelastic constitutive relations of SMA embedded sandwich structure for any k^{th} lamina is derived from the source [9] by incorporating the blocking stress phenomena and conceded in the following form:

$$\left\{\sigma_{Total}\right\}^k = \left[\bar{Q}\right]^k \left\{\varepsilon_{Total}\right\}^k + \left\{\sigma_{recovery}\right\}^k V_s^k - \left(\left[\bar{Q}\right]_m \left\{\alpha\right\}_m V_m\right)^k \Delta T \tag{4}$$

where, $\left\{\sigma_{recovery}\right\}$ the recovery stress generated in SMA fibre due to the temperature increment (ΔT) and the details regarding the mathematical constituents (volume fractions, reduced transformed stiffness component and strain tensor etc.) in Eq. (4) can be seen in the reference [9]. Additionally, ΔT is the change in temperature increment due to the uniform temperature environment.

Now, the total energy (U) expression including the work done (W) due to the resultant in-plane thermal forces of the composite sandwich plate including the recovery forces are presented in the following lines by substituting the corresponding stress and strain values.

$$U = \frac{1}{2}\int_v \left\{\varepsilon_{Total}\right\}^T \left\{\sigma\right\} dV \tag{5}$$

$$W = \frac{1}{2}\int_A \left\{\varepsilon_G\right\}^T \left[D_G\right] \left\{\varepsilon_G\right\} dA \tag{6}$$

where, $\left\{\varepsilon_G\right\}$ and $\left[D_G\right]$ are the corresponding geometrical and the material property matrix.

The FEM has been adopted in the present analysis due to known advantages i.e. easy adoptability and capable of solving the complex structural problem (geometry and material related). In this regard, an isoparametric nine-noded quadrilateral element with ten DOFs per node is implementated for the domain discretisation and the modified displacement field variable $\left\{\delta\right\}$ is expressed as:

$$\left\{\delta\right\} = \sum_{i=1}^{9} N_i \left\{\delta_i\right\} \tag{7}$$

where, $\left\{\delta_i\right\} = \left[u_{0i} \quad v_{0i} \quad w_{0i} \quad \theta_{1i} \quad \theta_{2i} \quad \theta_{3i} \quad \phi_{1i} \quad \phi_{2i} \quad \zeta_{1i} \quad \zeta_{2i}\right]^T$ is the nodal displacement filed vector and N_{i} is the interpolating functions associated with the 'i^{th} 'node.

Now, the modified form of the strain vector is rewritten after implementing nodal shape functions and represented as:

$$\left\{\bar{\varepsilon}\right\} = \left[B\right]\left\{\delta\right\} \tag{8}$$

where, [*B*] is the generic form of the strain displacement relations.

Similarly, the energy and the work done expressions are modified further by substituting the nodal shape function variable (Eq. 7) in Eqs. (5) and (6) and the elemental matrices provided in the following lines.

$$U^e = \frac{1}{2}\int_A \left(\{\delta\}_i^T [K]^e \{\delta\}_i \right) dA + \{F_{\Delta r}\}_i - \{F_{\Delta T}\}_i \tag{9}$$

$$W^e = \frac{1}{2}\int_A \left(\{\delta\}_i^T [K_G]^e \{\delta\}_i \right) dA \tag{10}$$

where, $[K]^e = \int_{-1}^{+1}\int_{-1}^{1} [B]_i^T [D][B]_i |J| d\xi d\eta$, $\{F_{\Delta r}\}^e = \int_A [B]_i^T \{N_{\Delta r}\} dA$, $\{F_{\Delta T}\}^e = \int_A [B]_i^T \{N_{\Delta T}\} dA$,

$[K_G]^e = \int_{-1}^{+1}\int_{-1}^{+1} [B_G]_i^T [D_G][B_G]_i |J| d\xi d\eta$. $[K_G]^e$ represents the elemental geometrical stiffness matrix and $[B_G]$ is similar to the strain-displacement matrix obtained due to the geometrical distortion under the elevated thermal loading.

Finally, the governing equation of the buckled laminated composite sandwich plate bonded with SMA fibre is derived by minimizing the total potential energy (TPE) functional and expressed as:

$$\delta \prod = 0 \tag{11}$$

where, $\prod = U^e + W^e$

Now, the final form of the eigenvalue equation of the buckled smart laminated sandwich composite plate is expressed in the following line by substituting Eqs. (9) and (10) in Eq. (11).

$$([K_S] - T_{cr}[K_G])\{\delta\} = 0 \tag{12}$$

where, $[K_S] = ([K] + [K_{recovery}])$ and $[K_G]$ are the global stiffness matrix and global geometrical stiffness whereas $[K_{recovery}]$ is the stiffness due to recovery stress behaviour of SMA. Additionally, T_{cr} represents the critical buckling temperature load.

3. Results and Discussion

The desired FE solutions for the thermal buckling load parameter of SMA bonded sandwich composite structure are obtained computationally via the suitable MATLAB code in association with higher-order model. In order to verify the stability and the degree of accuracy of the current numerical solution, the model is engaged to evaluate the buckling temperature for different mesh densities. Also, the values are compared with the published data. In this analysis, three different sets of end support conditions are utilized and provided in the following lines.

All edges clamped

$u_0 = v_0 = w_0 = \theta_1 = \theta_2 = \theta_3 = \phi_1 = \phi_2 = \zeta_1 = \zeta_2 = 0$ at $x = 0$, a and $y = 0$, b

All edges simply-supported (SS)

$v_0 = w_0 = \theta_2 = \theta_3 = \phi_2 = \zeta_2 = 0$ at $x = 0$, a

$u_0 = w_0 = \theta_1 = \theta_3 = \phi_1 = \zeta_1 = 0$ at $y = 0$, b

Two opposite edges clamped and simply-supported

$u_0 = v_0 = w_0 = \theta_1 = \theta_2 = \theta_3 = \phi_1 = \phi_2 = \zeta_1 = \zeta_2 = 0$ at $x = 0$, a

$u_0 = w_0 = \theta_1 = \theta_3 = \phi_1 = \zeta_1 = 0$ at $y = 0$, b

For the computation purpose, the following material parameters of SMA laminated composites Kumar and Singh [8] are utilised:

Composite matrix: (graphite/epoxy)

$E_1 = 155\times10^9\, N/mm^2; E_2 = 8.07\times10^9\, N/mm^2;\ G_{12} = G_{13} = 4.55\times10^9\, N/mm^2; G_{23} = 3.25\times10^9\, N/mm^2;$

$\upsilon_{12} = \upsilon_{13} = 0.22;\ \upsilon_{23} = 0.3488; \alpha_0 = 10^{-6}; \alpha_1 = -0.07\times\alpha_0; \alpha_2 = \alpha_3 = 30\times\alpha_0$

SMA fibres - Nitinol: E is obtained from Kumar and Singh [8] and Park *et al*. [6] depending on the temperature increment and the recovery stress is obtained from Park *et al*. [6] depending on the prestrain of the SMA fibres $(\varepsilon_r = 1\%)$ and the temperature increment.

$E_0 = 0.1\times10^9\, N/mm^2; G = 24.86\times10^9\, N/mm^2; \upsilon_{12} = 0.33; \alpha_1 = 10.26\times10^{-6}/^o C$

3.1 Convergence and validation study

In order to check the required convergence behaviour and the validity, a square simply-supported (45°/S/S/45°) laminated composite plate bonded with SMA fibre example is solved including the material properties as defined earlier. For the computation purpose, the volume fraction of SMA (V_S) fibre 0.1,

prestrain (ε_r) 1% and two length-to-thickness ratios (a/h = 50 and 100) are taken. In addition, the nondimensional critical buckling temperature is obtained using $T_{cr} = 10^3 \lambda \alpha_0 \Delta T$. Now, to check and demonstrate the convergence behaviour of the presently developed numerical model, the responses are obtained for a different number of elements and presented in Figure 2. From the figure, it is evident that the presently obtained results are showing very good rate of convergence with the mesh refinement. In this study, a (5×5) mesh size has been utilised for the computation of new results as well as the comparison purpose. The comparison study indicate an acceptable range of differences (≤10%) between the present and reference values.

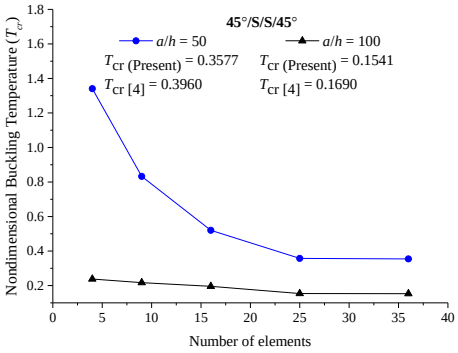

Figure 2. Convergence and comparison study of buckling temperature parameter

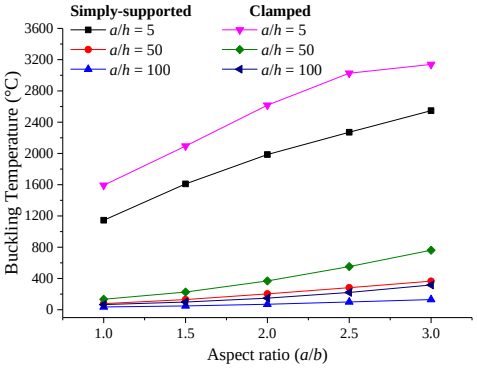

Figure 3. Effect of aspect ratios (a/b) on buckling temperature of sandwich plate embedded with SMA fibre (h_c/h_f = 25)

3.2 Numerical examples

The buckling responses are obtained for sandwich plate embedded with SMA fibre using different geometrical parameters and discussed in the detail in upcoming subsections. For the computation purpose, the SMA volume fraction (V_S) is considered as 0.1 and prestrain (ε_r) 1% until unless mentioned elsewhere. In the present research, the responses are obtained for (S/45°/-45°/C/-45°/45°/S) lamination scheme. It is important to mention that SMA properties for the present analysis are similar to the properties as mentioned in [8] whereas the material properties of the sandwich are taken same as [10]. The detailed properties of the face sheet and core layer of the sandwich construction are:

$$\text{Face sheet: } E_1 = 275\times10^9\, N/mm^2; E_2 = E_3 = 6.9\times10^9\, N/mm^2; G_{12} = G_{23} = G_{13} = 6.9\times10^9\, N/mm^2;$$
$$\upsilon_{12} = \upsilon_{13} = 0.25; \upsilon_{23} = 0.3$$
$$\text{Core: } E_1 = E_2 = E_3 = 0.5776\times10^9\, N/mm^2; G_{12} = G_{13} = 0.1079\times10^9\, N/mm^2; G_{23} = 0.22215\times10^9\, N/mm^2;$$
$$\upsilon_{12} = \upsilon_{23} = \upsilon_{13} = 0.0025$$

3.2.1 Buckling load variation due to change in aspect ratio (a/b)

The buckling temperature of SMA embedded sandwich plate is obtained for two different support conditions (SS and clamped) by varying five a/b = 1, 1.5, 2, 2.5 and 3 and three a/h = 5, 50 and 100 values. The temperature values are computed by taking the core-to-face thickness ratio as h_c/h_f = 25 and presented in Figure 3. The temperature parameter of the smart sandwich structure is increasing while the aspect ratios (a/b) increase whereas follow a reverse trend with a/h values. The responses are following an expected kind of behaviour i.e. the buckling temperature increase or decrease while the global structural stiffness values altered according to the related geometrical parameters (length-to-thickness ratio and aspect ratio) since it is directly proportional to the stiffness.

3.2.2 Variation of thermal buckling load due to different length-to-thickness ratio (a/h)

In this example, the buckling temperature of SMA embedded square sandwich plate is obtained to show the influence of the length-to-thickness ratios (a/h) and presented in Figure 4. For the computation purpose, two different support conditions (all edges simply supported and clamped) are considered with three core-to-face thickness ratios (h_c/h_f = 5, 15 and 25) and seven length-to-thickness ratios (a/h = 2, 5, 10, 15, 20, 25 and 50). From the figure, it is understood that the buckling temperature values are following the increasing trend for both the length-to-thickness ratios (a/h) as well as the core-to-face thickness ratios (h_c/h_f). The

reason behind this is already discussed earlier and it is well known that the a/h increases, the structure becomes thin and it can be buckle easily.

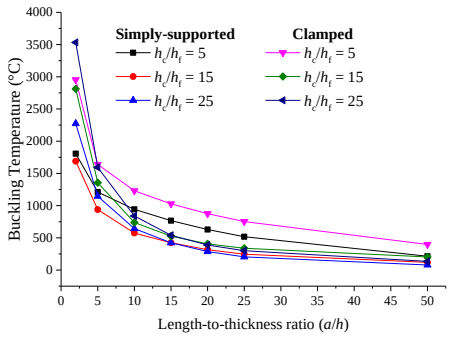

Figure 4. Variation of thermal buckling load parameter of SMA bonded sandwich plate due to different length-to-thickness ratios (a/h)

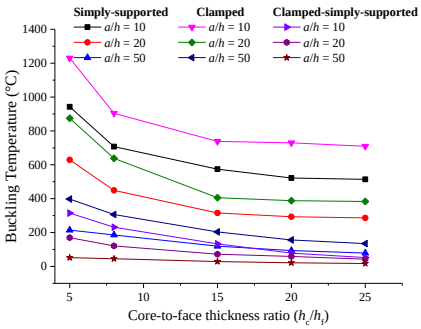

Figure 5. Core-to-face thickness ratio (h_c/h_f) influence on thermal buckling temperature of SMA bonded sandwich plate (a/b = 1)

3.2.3 Core-to-face thickness ratio (h_c/h_f) influence on thermal buckling

Now, one more example of square sandwich plate problem is solved for five, h_c/h_f = 5, 10, 15, 20 and 25 and presented in Figure 5. For the computational purpose, the necessary geometrical parameters are taken as: three length-to-thickness ratios (a/h = 10, 20 and 50) and three support conditions (SS, clamped and mixed). The buckling temperature curve is declining while the h_c/h_f value increases.

4. Conclusions

The buckling temperature of SMA embedded sandwich composite plate is obtained numerically via a suitable computer code in conjunction with the current higher-order kinematic model. The numerical model is developed by taking both the geometrical and material nonlinearity through the Green-Lagrange strain and marching technique. The final governing eigenvalue equations are solved using the isoparametric FEM steps and the correctness of the current numerical solutions verified by solving the adequate number of examples. After the necessary verification, the model is extended suitably to evaluate the influence of either one or more parameter on the buckling temperature parameter of SMA bonded sandwich structure including the recovery effect. The computed values indicate that the clamped sandwich structure show higher values of temperature load irrespective of geometrical parameters and SMA bonding.

References

[1] Rogers C A, Liang C and Jia J 1991 *Comput Struc* **38** 569–580
[2] Duan B, Tawfik M, Goek S N, Ro J J and Mei C 2000 *Proceedings of SPIE* **3991** 358–362
[3] Tawfik M, Ro J J and Mei C 2002 *Smart Mater Struct* **11** 297–307
[4] Zak A J, Cartmell M P, Ostachowicz W M and Wiercigroch M 2003 *Smart Mater Struct* **12** 338–346
[5] Shiau L C and Kuo S Y 2004 *Mech Based Des Struct Mach* **32** 57–72
[6] Park J S, Kim J H and Moon S H 2004 *Compos Struct* **63** 179–188
[7] Kuo S Y, Shiau L C and Chen K H 2009 *Compos Struct* **90** 188–195
[8] Kumar S K and Singh B N 2009 *J Aerosp Eng* **22** 342–353
[9] Panda S K and Singh B N 2013 *Aerosp Sci Technol* **29** 47–57
[10] Dehkordia M B and Khalili S M R 2015 *Compos Struct* **123**, 408-419
[11] Katariya P V, Panda S K, Hirwani C K, Mehar K and Thakare O 2017 *Smart Struct Syst* **20** 595–605